

# A facile process for preparing superhydrophobic PBZ-PTFE coating with excellent stable properties

Sheng Lei<sup>1</sup> · Zhongqi Shi<sup>1</sup> · Junfei Ou<sup>2</sup> · Wen Li<sup>2</sup> · Guanjun Qiao<sup>3</sup> · Xinhua Yu<sup>4</sup>

Received: 14 June 2016 / Accepted: 19 October 2016 / Published online: 10 November 2016  
© Springer-Verlag Berlin Heidelberg 2016

**Abstract** We present a facile way to fabricate superhydrophobic PBZ-PTFE coating which can be easily prepared in large scale. The superhydrophobic PBZ-PTFE coating was prepared by spraying the PTFE condensed dispersion solution and the benzoxazine mixture solution on the substrate. The water contact angle on the prepared coating reaches 166.5°, and the sliding angle is only 1°. The PTFE weight fraction is optimized to 60% which provides high surface roughness of 3.54 μm required for superhydrophobicity. Importantly, the superhydrophobic coating exhibits excellent temperature stability and corrosion resistance. In addition, the stability of the superhydrophobic coating was evaluated by adhesive tape peeling experiment, bend test, crosscut test and water impact test. We expect that this fabrication technique will have great prospects for industrial applications.

## 1 Introduction

It is fascinating that the water drops keep the sphere shape on the lotus leaves and can be easily rolled without adhesion. This special phenomenon of surface wettability is known as the superhydrophobic surface which also exists on rose petals [1], insect wings [2] and legs of the water strider [3] in nature. The superhydrophobic surfaces exhibiting a static water contact angle (CA) greater than 150° and a sliding angle (SA) less than 10° have become an attractive subject for both academic research and industrial applications over the years [4–7]. It has a wide variety of practical applications in daily life, industry and agriculture for their particular characteristics, such as self-cleaning [8–10], corrosion resistance [11, 12], anti-icing [13, 14] and oil-water separation [15–17].

There are two main ways to fabricate artificial superhydrophobic surfaces. One is to modify a rough surface by compounds with low surface free energy and the other is to create a rough structure on a hydrophobic surface [18–20]. Inspired by these two standards, various techniques to fabricate artificial superhydrophobic surfaces have been developed in the last decades. However, most of the artificial superhydrophobic surfaces are limited in practical applications due to the thermal instability and poor mechanical properties.

It is well known that the polytetrafluoroethylene (PTFE) is an attractive material with the low surface free energy, high and low temperature resistance, excellent chemical inertness and abundant availability [21–24]. Polybenzoxazines (PBZ), a newly developed polymer material with a low surface free energy, has many unique properties such as the low water absorption, high glass transition temperature and excellent resistance to heat [25–28].

---

**Electronic supplementary material** The online version of this article (doi:10.1007/s00339-016-0514-9) contains supplementary material, which is available to authorized users.

---

✉ Wen Li  
wenl@ualberta.ca

✉ Guanjun Qiao  
gjiao@ujs.edu.cn

<sup>1</sup> State Key Laboratory for Mechanical Behavior of Materials, Xi'an Jiaotong University, Xi'an 710049, China

<sup>2</sup> School of Materials Science and Engineering, Nanchang Hangkong University, Nanchang 330063, China

<sup>3</sup> School of Materials Science and Engineering, Jiangsu University, Zhenjiang 212013, China

<sup>4</sup> Jiangxi Ganyue Expressway CO., LTD, Nanchang 330025, China

In this paper, we present a simple and feasible method for constructing a composite PBZ-PTFE coating by spraying on the substrates of glass and stainless steel. It is found that the so-prepared coating not only has the property of superhydrophobicity but also possesses the excellent temperature stability, mechanical stability and corrosion resistance.

## 2 Experimental

### 2.1 Materials

2,2-bis(3-phenyl-3,4-dihydro-2H-1,3-benzoxazinyl)propane (BA-a benzoxazine) was purchased from Shanghai Pingxiu Co., Ltd., China. The polytetrafluoroethylene (PTFE) con-

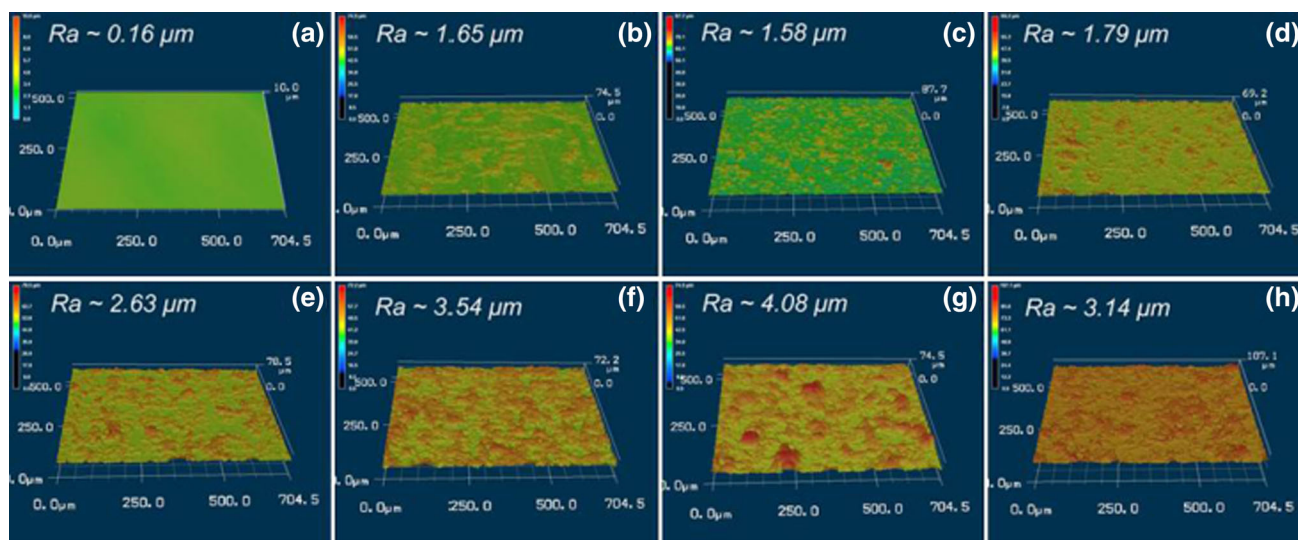


**Fig. 1** Laser microscopy images of the PBZ-PTFE coatings on glass substrate. The PTFE weight fraction is: **a** 0, **b** 23.1%, **c** 37.5%, **d** 47.4%, **e** 54.5%, **f** 60%, **g** 64.3% and **h** 70.5%

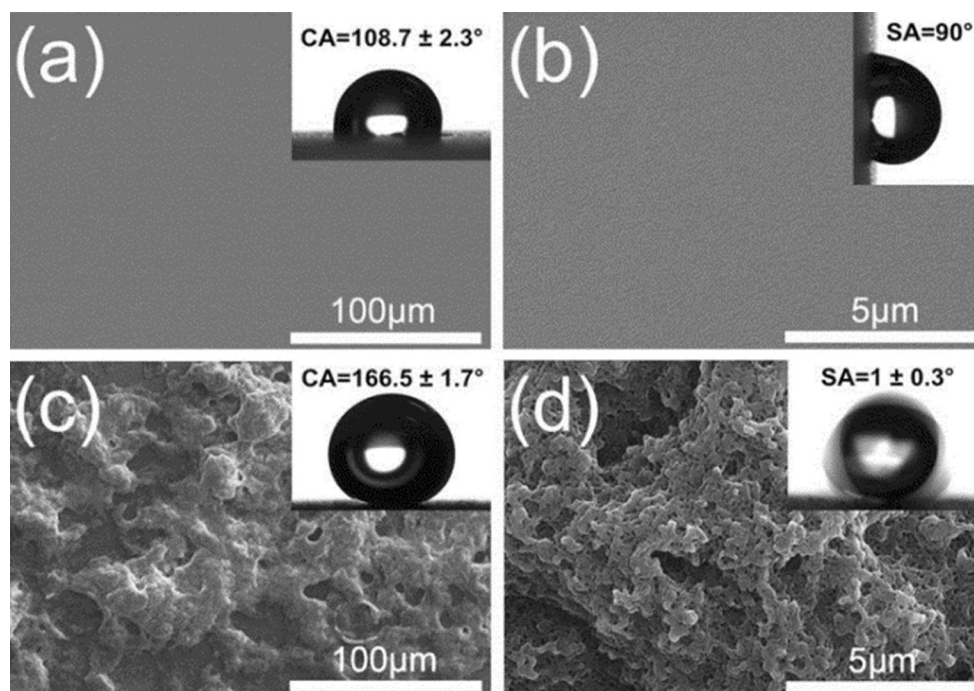


**Fig. 2** FESEM images of the PBZ-PTFE coatings on glass substrate. The PTFE weight fraction is: **a**, **b** 0 wt% and **c**, **d** 60 wt%. The *inset* shows the optical images of the water contact angle and sliding angle

densed dispersion solution was obtained from Shenzhen Kejing Co., Ltd., China. The PTFE solid content is up to 60% and the particle size is 50 nm. The specific gravity of PTFE solution is 1.5 g/cm<sup>3</sup>. Stainless steel (100 × 50 × 0.5 mm) and glass (75 × 25 × 2 mm) were used as the substrate. Stainless steels were supplied by Shenzhen Advanced Metal Co., Ltd., China. Glass was obtained from the Sinopharm Chemical Reagent Co., Ltd., China. Absolute ethyl alcohol, hydrochloric acid and acetone were purchased from Shanghai Chemical Reagent Co., Ltd., China. All chemical reagents were of analytical grade. Deionized water was exclusively used in all aqueous solutions and rinsing procedures.

## 2.2 Preparation of superhydrophobic PBZ-PTFE coatings

The superhydrophobic polybenzoxazines coatings were fabricated by using the method of spray coating. At first, 1.5 g of benzoxazine was dissolved in 100 mL acetone. Then, the PTFE condensed dispersion solution was gradually added to the above solution and stirred magnetically for 10 min. The substrates were ultrasonically cleaned with hydrochloric acid, acetone and ethyl alcohol in turn. To prepare a coating, the suspension solution was sprayed on glass or stainless steel at a flow rate of 1.6 mL/s by a spray gun (nozzle diameter, 1.0 mm) with a compressed air pressure of 0.3 MPa. The distance between the nozzle head and the sample was approximately 20 cm. The spray coating was repeated 2–5 times until the surface was covered with a film of uniform thickness. Finally, the prepared coating was air-dried at 200 °C for 10 min in an oven.

## 2.3 Characterizations

The morphology of the as-prepared coatings was determined by a field emission scanning electron microscope (FESEM, FEI Nova NanoSEM 450, America) at 5–15 kV under vacuum environment. The surface topography and roughness of the coatings were measured with a confocal laser scanning microscope (Keyence, VK-9700). The average surface roughness of each sample was measured in 500 × 500 μm<sup>2</sup> planar for at least three different positions. The thermal properties of the coatings were explored by a thermogravimetric analyzer (TGA, 209 F1, Germany) with a heating rate of 10 °C/min under air atmosphere. An optical contact angle meter (DSA 100, Krüss, Germany) was used to analyze the water contact angle and sliding angle with the volume of the water droplets being 6 μL at ambient temperature. The average water contact angle and sliding angle values were obtained by measuring the same sample in at least five different positions.

## 3 Results and discussion

The PTFE concentration plays a crucial role in the influence on the surface microstructure and surface roughness. Figure 1 shows the three-dimensional surface topography of the samples with different weight fraction of PTFE (wt% of PTFE), which can be calculated by the following equation:

$$\text{Wt\% of PTFE} = \frac{m_{\text{PTFE}}}{m_{\text{PTFE}} + m_{\text{PBZ}}}$$

where  $m_{\text{PTFE}}$  and  $m_{\text{PBZ}}$  presents the solid weight of PTFE and PBZ, respectively. The surface of Fig. 1a is very smooth and the surface roughness is only 0.16 μm. It is different from that of the rest of the samples (Fig. 1b–h) because of the absence of PTFE. The surface roughness is remarkably increased to 1.65 μm when small amount of PTFE is added (23.1 wt%, Fig. 1b), whereas there are many gaps between particles. After adding 37.5 wt% of PTFE, the surface roughness is slightly reduced to 1.58 μm (Fig. 1c). The PTFE particles are more uniformly, although they do not cover the entire area. When the PTFE weight fraction increases from 47.4 to 54.5, 60 and 64.3%, the surface roughness rapidly increases from 1.79 to 2.63, 3.54 and 4.08 μm, respectively. However, when the PTFE weight fraction further increases to 70.5 wt%, the surface is completely covered by PTFE aggregate particles and the surface roughness slightly decreased to 3.14 μm. This indicates that the surface roughness of the coating is closely related to the content of PTFE particles.

To get more information on the surface morphology, Fig. 2 shows the FESEM images of the samples. The pure PBZ surface shows a very smooth morphology (Fig. 2a, b), while the PBZ-PTFE coating with 60 wt% of PTFE gets much rougher (Fig. 2c, d). It is more clearly observed that a large number of PTFE particles cluster together and honeycomb-like rough microstructures with many voids

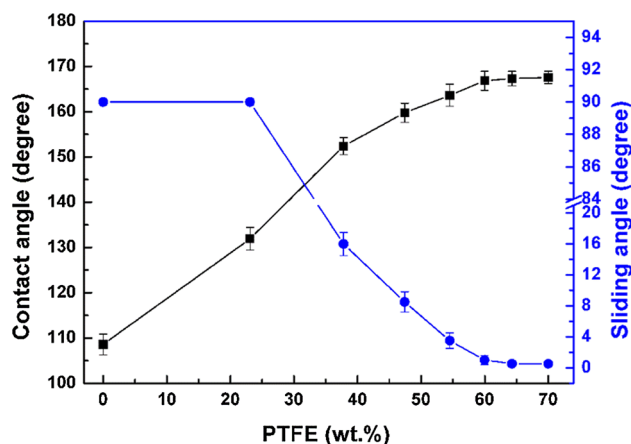


**Fig. 3** Water contact angles and sliding angles for the PBZ-PTFE coatings on glass substrate with different PTFE weight fraction

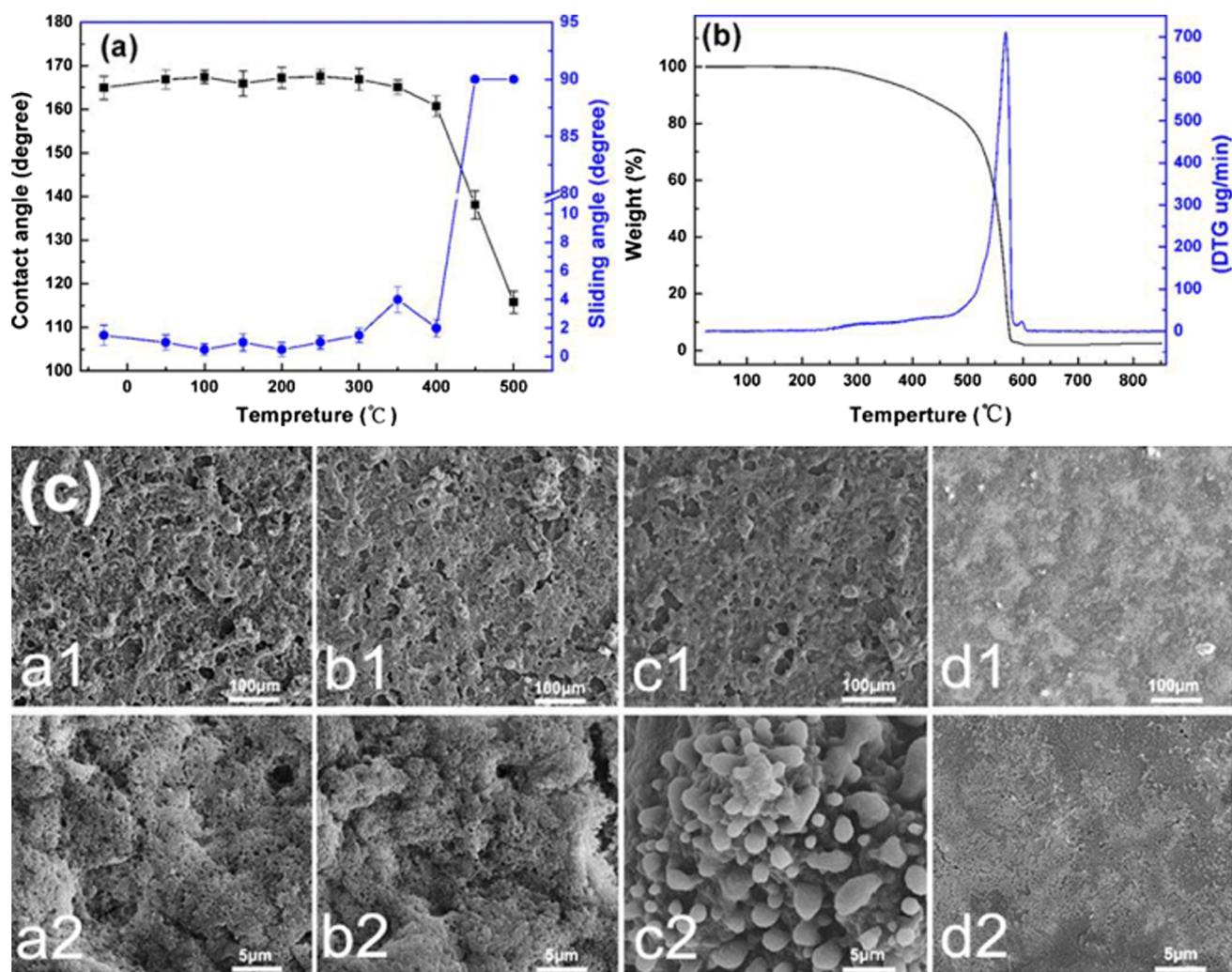


**Fig. 4** **a** Water contact angles and sliding angles for the PBZ-PTFE coatings (the PTFE weight content is 60%) on glass substrate after exposed to different temperatures for 1 h. **b** Differential scanning

calorimetric analysis of the coating. **c** FESEM images of the PBZ-PTFE coatings after annealing at different temperature: 200 °C (*a1*, *a2*); 300 °C (*b1*, *b2*); 400 °C (*c1*, *c2*) and 500 °C (*d1*, *d2*)

form. This hierarchical microstructure could effectively increase the roughness of the surface and trap air in voids, which increases the interface between air and water promoting the superhydrophobicity.

The water contact angle (CA) and sliding angle (SA) for PBZ-PTFE coatings is presented in Fig. 3. For the pure PBZ surface [25], the CA is measured to be  $108.7 \pm 2.3^\circ$  (Figs. 2a inset, 3) and SA is  $90^\circ$  (Figs. 2b inset, 3). After 23.1 wt% of PTFE was added, the CA increases to  $131.9 \pm 2.5^\circ$  and SA remains  $90^\circ$ . This is probably because there are a lot of big gaps and voids on the surface (Fig. 1a) and consequently the water droplets can easily sink into the surface and are difficult to roll away, displaying the Wenzel's wetting state [6]. A superhydrophobic state with a CA of  $153.4 \pm 1.6^\circ$  and SA of  $16 \pm 1.4^\circ$  is obtained by increasing the PTFE weight fraction to 37.5%. This suggests that the PTFE particles can enhance the

surface roughness and reduce the surface energy simultaneously, and the surface wettability switches from the hydrophobic Wenzel state to the superhydrophobic Cassie–Baxter state [7]. As the PTFE weight fraction further increased to 47.4, 54.5 and 60%, the CAs of the coatings increase gradually to  $159.7 \pm 1.9^\circ$ ,  $163.6 \pm 2.1^\circ$  and  $166.5 \pm 1.7^\circ$ , respectively, while the SAs reduce gradually to  $8.5 \pm 1.1^\circ$ ,  $3.5 \pm 0.8^\circ$  and  $1 \pm 0.3^\circ$ , respectively. However, as the PTFE content further increased to 64.3% and even to 70.5%, the values of CA and SA vary very little. The maximum value of CA can reach  $167.6^\circ$ , and the SA is approximately  $0.5^\circ$ . It is demonstrated that the PTFE for the superhydrophobicity is optimized to be 60 wt% (Fig. 3).

The PBZ-PTFE coating on glass substrate is exposed to different temperatures for 1 h. Then, the coatings are taken out and exposed to the room temperature for 1 h. After

such thermal treatment, the surface wettability (Fig. 4a) and surface morphology (Fig. 4c) of the coatings are measured. It indicates that, in the temperature range of  $-30 \sim 400$  °C, the thermal treatment has little influence on the surface wettability. However, after heat treatment at 450 or 500 °C, the CAs decrease quickly to  $138.1 \pm 3.2^\circ$  and  $115.8 \pm 2.5^\circ$ , respectively. Water droplet is difficult to roll away from the surface and SAs are  $90^\circ$ . In the aspect of the surface morphology, after treated at 200 and 300 °C, the difference is very small. After annealed at 400 °C for 1 h, some microparticles clusters appeared on the surface.

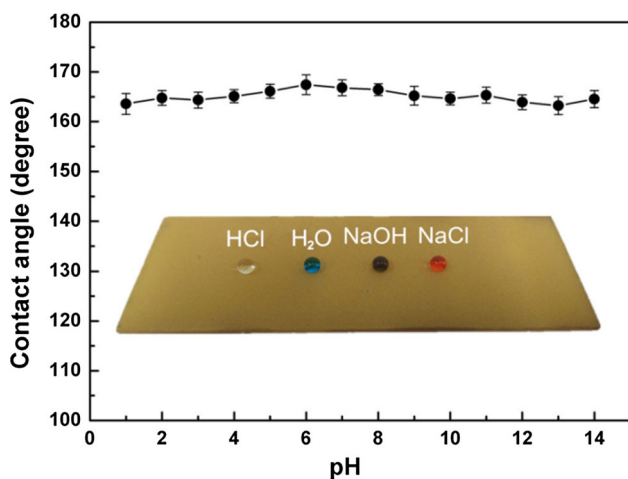


**Fig. 5** Relationship between pH and the water contact angle of the PBZ-PTFE coating (the PTFE weight content is 60%) on the glass substrate. The inset photograph shows  $H_2O$ , HCl, NaOH and NaCl solution on the coating

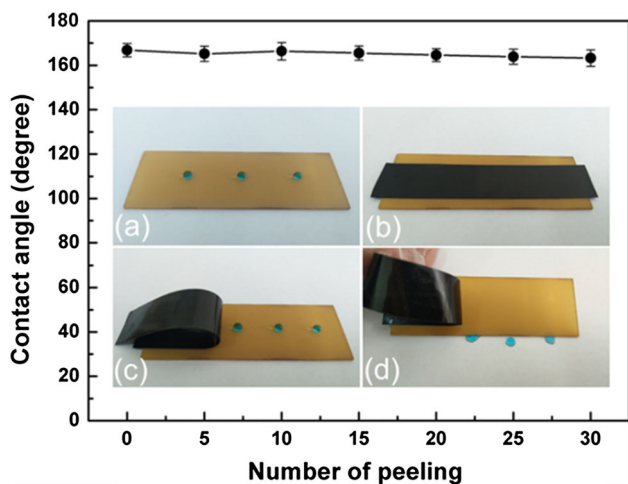


**Fig. 6** Water contact angle of the PBZ-PTFE coatings (the PTFE weight content is 60%) on the glass substrate treated by adhesive tape peeling tests. The inset depicts the adhesive tape peeling test process: **a** the PBZ-PTFE coating before test; **b** the adhesive tape was pasted onto the surface; **c** the adhesive tape was peeled off partially, and water droplets were dripped thereon; **d** the adhesive tape was pulled off slightly, and the water droplets rolled off easily

This was probably because the PTFE nanoparticles tended to merge into micro-ones. However, after annealed at 500 °C for 1 h, the surface became much smoother. This is probably because, at temperature approximately 500 °C, PBZ and PTFE will decompose [29, 30]. Thermal stability of the PBZ-PTFE coating was explored under air atmosphere and, the TGA and DTG curves are shown in Fig. 4b. The weight of the coating almost does not change when the temperature is lower than 300 °C. As the thermally treated temperature increased from 300 to 500 °C, the weight loss increases slowly: 5% (350 °C), 8.5% (400 °C), 14% (450 °C) and 20% (500 °C). For the temperature above 500 °C, the weight loss of the PBZ-PTFE coating becomes much more apparent. In DTG curve, there is an obvious exothermic peak at 568 °C attributing to the maximum rate of decomposition occurs.

The so-prepared superhydrophobic coatings (PBZ-PTFE coatings with the PTFE weight content of 60%) on glass substrates were immersed into different aqueous solutions for 24 h with the pH range from 1 to 14 (the pH was adjusted by HCl or NaOH). Then, the surface wettability was tested (Fig. 5). It was found that the superhydrophobic coatings show excellent stability and all the CAs are above  $160^\circ$ . The inset photograph shows the pure water, hydrochloric acid (1 M), sodium hydroxide (1 M) and sodium chloride (3.5 wt%) aqueous solution still keep spheres on the coating and can roll away easily when the surface is slightly tilted. These results suggest that the coatings have excellent corrosion resistance and can be used in a broad pH range of corrosive water.

An adhesive tape peeling test was performed on the coating by a 3 M adhesive tape with the adhesion force of 0.44 N/mm (Fig. 6). The water droplets are in spherical shape on the surface. The adhesive tape peeling test was repeated more than 30 times and it was found that the CA remains above  $160^\circ$  and the water droplets move quickly when the surface is slightly tilted.

To estimate the adhesion strength between the superhydrophobic coating and the substrate, the PBZ-PTFE coatings (the PTFE weight content is 60%) on the stainless steel substrate are completely bended and then returned to the original state. This bending and recovering process is set as one cycle. After 10 cycles, the water droplets still keep the spherical shape in the folded area (Fig. 7a). To observe the surface features of the folded area, the coating is examined by FESEM and it is found that a microgroove with a width of approximately 20  $\mu\text{m}$  appears (Fig. 7d). However, the coating in the adjacent area remains intact (Fig. 7c). The adhesion strength of the coating is also evaluated by the crosscut test according to the Chinese standard GB9286-98, which is consistent with ISO-2409. The test results indicate that the coating adhesion strength is level 0. Moreover, the FESEM image shows the cutting

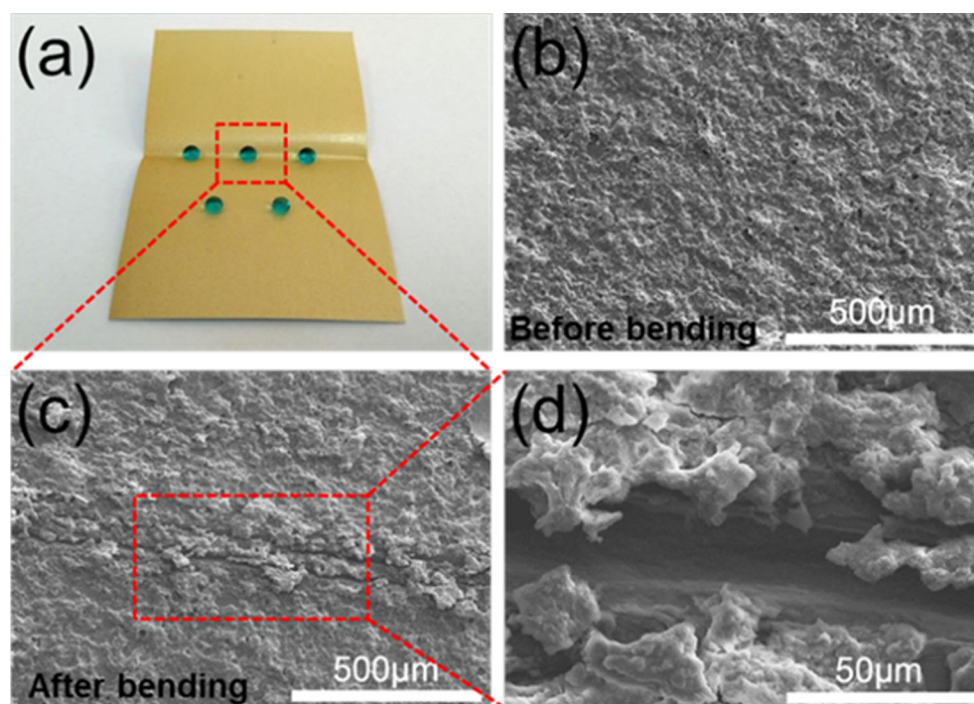


**Fig. 7** **a** Photograph of water drops on the PBZ-PTFE coatings (the PTFE weight content is 60%) on the stainless steel substrate after bending tests for 10 cycles. **b** FESEM images of the coating before

bending. **c** FESEM images of the coating after bending for 10 cycles. **d** High magnification of the image (c)

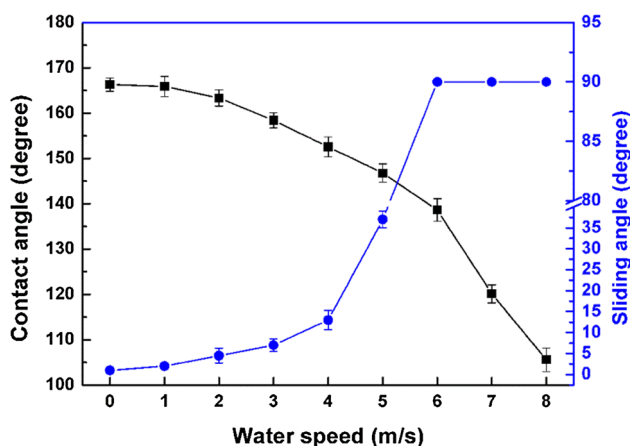


**Fig. 8** Water contact angles and sliding angles of the PBZ-PTFE coatings (the PTFE weight content is 60%) on the glass substrate with water speed

edge is smooth and without peeling coating (Figure S1). These results demonstrated the strong adhesion strength between the coating and the substrate.

The stability of the superhydrophobic coatings is further measured by the water impact test using a self-made device (Figure S2). The water flow at a different speed from 350 mm height dashes onto the coating. The CAs of the coating are detected after continuous water flow impacting for 15 min. Figure 8 presents the variation of CAs with different water flow speeds. The coatings maintain

superhydrophobicity at the water flow speed less than 4 m/s. With the water flow speed of 5 m/s, the CA decreases to  $145.8 \pm 3.7^\circ$  and SA increases to  $38 \pm 2.9^\circ$ . This is because, as the water flow becomes faster, the impact pressure on the superhydrophobic surface becomes larger and the water replaces the trapped air with the voids in the rough surface of coating. This test indicates that the coating has a good stability under the condition of low water flow speed impact.

## 4 Conclusions

In summary, the superhydrophobic PBZ-PTFE coating was prepared by the method of spraying. A mixture of benzoxazine and PTFE coating was transformed to the superhydrophobic PBZ-PTFE coating after heat treatment at  $200^\circ\text{C}$  for 10 min. The superhydrophobic property of the coating is gradually enhanced as the PTFE content increases. The PTFE weight fraction is optimized to 60% which provides a water contact angle as high as  $166.5^\circ$  and a sliding angle as low as  $1^\circ$ . The superhydrophobic property of the PBZ-PTFE coating can be retained by exposing it to harsh environments, such as low/high temperatures ( $-10$  to  $400^\circ\text{C}$ ), acid/basic aqueous solutions (pH range from 1 to 14), mechanical bending (10 cycles) and cutting (crosscut test, level 0), and water flow impacting (water

flow speed less than 4 m/s). It is believed that such stable superhydrophobic coating may have important potential applications.

**Acknowledgements** The work was supported by the International S&T Cooperation Program of China (Grant 2012DFA51200) and the Defense Industrial Technology Development Program (A0520110009).

## References

- M. Jin, X. Feng, L. Feng, T. Sun, J. Zhai, T. Li, L. Jiang, Superhydrophobic aligned polystyrene nanotube films with high adhesive force. *Adv. Mater.* **17**, 1977–1981 (2005)
- L. Feng, Y.A. Zhang, J.M. Xi, Y. Zhu, N. Wang, F. Xia, L. Jiang, Petal effect: a superhydrophobic state with high adhesive force. *Langmuir* **24**, 4114–4119 (2008)
- X.F. Gao, L. Jiang, Biophysics: water-repellent legs of water striders. *Nature* **432**, 36 (2004)
- A. Nakajima, A. Fujishima, K. Hashimoto, T. Watanabe, Preparation of transparent superhydrophobic boehmite and silica films by sublimation of aluminum acetylacetonate. *Adv. Mater.* **11**, 1365–1368 (1999)
- S. Herminghaus, Roughness-induced non-wetting. *Europhys. Lett.* **79**, 59901 (2007)
- R.N. Wenzel, Resistance of solid surfaces to wetting by water. *Ind. Eng. Chem. Res.* **28**, 988–994 (1936)
- A.B.D. Cassie, Contact angles. *Discuss. Faraday Soc.* **3**, 11–16 (1948)
- H.L. Liu, P.C. Zhang, M.J. Liu, S.T. Wang, L. Jiang, Organogel-based thin films for self-cleaning on various surfaces. *Adv. Mater.* **25**, 4477–4481 (2013)
- Z.G. Guo, F. Zhou, J.C. Hao, W.M. Liu, Stable biomimetic superhydrophobic engineering materials. *J. Am. Chem. Soc.* **127**, 15670–15671 (2005)
- W.S.Y. Wong, Z.H. Stachurski, D.R. Nisbet, A. Tricoli, Ultradurable and transparent self-cleaning surfaces by large-scale self-assembly of hierarchical interpenetrated polymer networks. *ACS Appl. Mater. Inter.* **8**, 13615–13623 (2016)
- P.M. Barkhudarov, P.B. Shah, E.B. Watkins, D.A. Doshi, C.J. Brinker, J. Majewski, Corrosion inhibition using superhydrophobic films. *Corros. Sci.* **50**, 897–902 (2008)
- F. Zhang, S.G. Chen, L.H. Dong, Y.H. Lei, T. Liu, Y.H. Yin, Preparation of superhydrophobic films on titanium as effective corrosion barriers. *Appl. Surf. Sci.* **257**, 2587–2597 (2011)
- M. He, J. Wang, H. Li, Y. Song, Super-hydrophobic surfaces to condensed micro-droplets at temperatures below the freezing point retard ice/frost formation. *Soft Matter* **7**, 3993–4000 (2011)
- A. Davis, Y.H. Yeong, A. Steele, I.S. Bayer, E. Loth, Superhydrophobic nanocomposite surface topography and ice adhesion. *ACS Appl. Mater. Inter.* **6**, 9272–9279 (2014)
- Q.M. Pan, M. Wang, Miniature boats with striking loading capacity fabricated from superhydrophobic copper meshes. *ACS Appl. Mater. Inter.* **2**, 420–423 (2009)
- J. Li, D.M. Li, Y.X. Yang, J.Q. Li, F. Zha, Z.Q. Lei, A prewetting induced underwater superoleophobic or underoil (super) hydrophobic waste potato residue-coated mesh for selective efficient oil/water separation. *Green Chem.* **18**, 541–549 (2016)
- D.D. Nguyen, N.H. Tai, S.B. Leea, W.S. Kuo, Superhydrophobic and superoleophilic properties of graphene-based sponges fabricated using a facile dip coating method. *Energy Environ. Sci.* **5**, 7908–7912 (2012)
- J.P. Zhang, S. Seeger, Polyester materials with superwetting silicone nanofilaments for oil/water separation and selective oil absorption. *Adv. Funct. Mater.* **21**, 4699–4704 (2011)
- S. Wang, L. Jiang, Definition of superhydrophobic states. *Adv. Mater.* **19**, 3423–3424 (2007)
- S.M. Kang, S. Hwang, S.H. Jin, C.H. Choi, J.M. Kim, B.J. Park, D. Lee, C.S. Lee, A rapid one-step fabrication of patternable superhydrophobic surfaces driven by Marangoni instability. *Langmuir* **30**, 2828–2834 (2014)
- S.R. Coulson, I. Woodward, J.P.S. Badyal, Super-repellent composite fluoropolymer surfaces. *J. Phys. Chem. B* **104**, 8836–8840 (2000)
- J.S. Bergström, L.B. Hilbert Jr., A constitutive model for predicting the large deformation thermomechanical behavior of fluoropolymers. *Mech. Mater.* **37**, 899–913 (2005)
- T.S. Sasikalaa, M.T. Sebastian, Mechanical, thermal and microwave dielectric properties of Mg<sub>2</sub>SiO<sub>4</sub> filled Polytetrafluoroethylene composites. *Ceram. Inter.* **6**, 7551–7563 (2016)
- Z. Zhang, X. Chen, Multiaxial ratcheting behavior of PTFE at room temperature. *Polym. Test.* **3**, 288–295 (2009)
- C.F. Wang, Y.C. Su, S.W. Kuo, C.F. Huang, Y.C. Sheen, F.C. Chang, Low-surface-free-energy materials based on polybenzoxazines. *Angew. Chem. Int. Ed.* **45**, 2248–2251 (2006)
- L.P. Yang, A. Raza, Y. Si, X. Mao, Y.W. Shang, B. Ding, J.Y. Yud, S.S. Deyab, Synthesis of superhydrophobic silica nanofibrous membranes with robust thermal stability and flexibility via in situ polymerization. *Nanoscale* **4**, 6581–6587 (2012)
- C.S. Liao, C.F. Wang, H.C. Lin, H.Y. Chou, F.C. Chang, Tuning the surface free energy of polybenzoxazine thin films. *J. Phys. Chem. C* **112**, 16189–16191 (2008)
- C.F. Wang, Y.T. Wang, P.H. Tung, S.W. Kuo, C.H. Lin, Y.C. Sheen, F.C. Chang, Stable superhydrophobic polybenzoxazine surfaces over a wide pH range. *Langmuir* **22**, 8289–8292 (2006)
- Y.S. Zheng, Y. He, Y.Q. Qing, Z.H. Zhuo, Q. Mo, Formation of SiO<sub>2</sub>/polytetrafluoroethylene hybrid superhydrophobic coating. *Appl. Surf. Sci.* **258**, 9859–9863 (2012)
- X.G. Teng, C. Sun, J.C. Dai, H.P. Liu, J. Su, F.Q. Li, Solution casting nafion/polytetrafluoroethylene membrane for vanadium redox flow battery application. *Electrochim. Acta* **88**, 725–734 (2013)